# Attosecond Correlation Dynamics

M. Ossiander[1,2,†], F. Siegrist[1,2], V. Shirvanyan[1,2], R. Pazourek[3], A. Sommer[1], T. Latka[1,2], A. Guggenmos[1,5], S. Nagele[3], J. Feist[4], J. Burgdörfer[3], R. Kienberger[1,2], M. Schultze[1,5,†]

1 Max-Planck-Institut für Quantenoptik, Hans-Kopfermann-Str. 1, 85748 Garching, Germany

2 Physik-Department, Technische Universität München, James-Franck-Str. 1, 85748 Garching, Germany

3 Institute for Theoretical Physics, Vienna University of Technology, Wiedner Hauptstrasse 8-10, 1040 Vienna, Austria

4 Departamento de Física Teórica de la Materia Condensada and Condensed Matter Physics Center (IFIMAC), Universidad Autónoma de Madrid, 28049 Madrid, Spain

5 Fakultät für Physik, Ludwig-Maximilians-Universität München, Am Coulombwall 1, 85748 Garching, Germany

†correspondence to: marcus.ossiander@mpq.mpg.de, martin.schultze@mpq.mpg.de

**Photoemission of an electron after a multi-electron system has absorbed a photon is commonly treated as one-particle phenomenon. Here we show how attosecond streaking spectroscopy in helium unveils the breakdown of this single-active-electron approximation by recording up to 6 attoseconds retardation of the dislodged photoelectron due to the influence of electronic correlations. We measure the photon-energy-dependent emission timing of electrons liberated from the helium ground state by a ~100 eV photon, either leaving the ion in its ground state or exciting it into a shake-up state. The study identifies an optical field driven DC-Stark-shift of charge-asymmetric ionic states formed after the entangled photoemission as key contribution to the observed correlation time shift and provides means towards complete wavepacket reconstruction. The sub-attosecond agreement with the predictions of quantum mechanical ab-initio modelling allows to determine the absolute zero of time in the photoelectric effect to a precision better than $^{1}/_{25}$–th of the atomic unit of time.**

Photoemission of an electron occurs when the energy $E_\gamma$ of the absorbed photon surpasses the ionization potential $IP$ of the illuminated system. This hypothesis marks the foundation of quantum mechanics[1] and the process was tacitly regarded as instantaneous until the tools of attosecond time resolved spectroscopy started to challenge this simplification about a century after the photoelectric effect was

postulated. When first experiments produced evidence for a delay in photoemission[2–5], it was recognized with recourse to a theoretical debate in the 1950s that the movement of the ionized electronic wavepacket through the attractive ionic potential can be interpreted as a (half-)scattering process leading to an energy dependent phase shift as compared to its free movement in vacuum[6–8]. Such a phase shift translates to the retardation or advance of the wavepacket[9–11], potentially observable as a delay in time-resolved experiments. Since this (positive or negative) delay became an experimental observable it poses a novel challenge for theory, resulting in a lively debate, see e.g.[12–24] and references therein. Even though both, experimental methodology and theoretical treatment, are still in their infancy, the experimental observations could be explained qualitatively by a variety of theoretical approaches. The lack of quantitative agreement was attributed to the missing or incomplete description of electronic correlation in the theoretical approaches and the presence of the strong laser field in the measurements that transiently modifies the ionic potential and the kinetics of the liberated wavepacket. Theory also indicated that a modification of the observed time shifts can arise from minute differences in the polarization of different states which in turn can exert a back-action on the outgoing electronic wavepacket[17,21,25].

An ideal test case for the experimental resolution of this somewhat inextricable situation and the investigation of the role of electronic correlations is single photon (shake-up) ionization of helium as sketched in Fig 1. For the direct photoionization process, the outgoing photoelectron is promoted into the ionization continuum with kinetic energy $E_{kin} = E_\gamma - IP^{He}$, (ionization energy of helium $IP^{He} = 24.6\,eV$) leaving the remaining electron more strongly bound in the $He^+$ ground state (shake-down). Alternatively, for sufficiently energetic photons ($E_\gamma > 65.5\,eV$) the electron remaining bound to the ion can be excited into one out of a series of ionic Rydberg states (shake-up (SU), or

correlation sattelites[26]) with excitation energies $\Delta E_{n=2}^{su} = 40.8$ eV (47.5, 50.2, 52.4,.. eV for $n = 3,4,5,..$) converging towards the second ionization limit. The first process, also referred to as direct photoionization, can be described to a good degree of approximation within a single particle framework, while the latter requires the interaction of both electrons and is a prototypical electronic correlation process. Such correlations evolve on the fast-paced attosecond timescale of electron dynamics and a measurement capable of resolving them would allow to isolate and explore the role of electronic correlations in the photoelectric effect and provide a benchmark for the refinement of high-level many-electron quantum theories.

The only multi-electron system for which the time-dependent Schrödinger equation including the quantum mechanical dynamics of all electrons in the presence of a laser field can be solved exactly is helium[12]. For all heavier elements the inner electrons residing with the ion can only be accounted for approximately, e.g., by density functional theories or Hartree-Fock methods[24]. Such approximate methods to describe electronic correlations limit the accuracy of the results obtained.

Earlier experimental studies of helium remained inconclusive due to the low photoabsorption cross section at photon energies relevant for attosecond spectroscopy and low photon flux sources resulting in large measurement uncertainties. Here we demonstrate how the advances of attosecond source technology now allow scrutinizing the role of multi-electron interactions in the photoelectric effect. To our knowledge, this constitutes the first experimental study achieving both sub-attosecond precision and accuracy evidenced by the near-perfect agreement with theory.

## Observation of the relative photoemission timing

To explore the timing of helium photoelectrons we perform pump-probe experiments according to the attosecond streak camera scheme[27], where an isolated attosecond pump pulse liberates an electron in the presence of a laser electric field. The characteristic laser induced modification of the photoelectron's kinetic energy depending on the arrival time difference between the two pulses can be used to track electronic processes with attosecond temporal resolution.

In a first step we generate trains of extreme-ultraviolet (XUV) attosecond bursts by frequency-upconversion of carrier-envelope-phase-stabilized, few-cycle, near infrared laser pulses (1.2 mJ, 3.9 fs)[28] via high-order harmonic generation (HHG) in neon[29,30]. Isolated attosecond pulses are selected through spectral filtering of the XUV pulses achieved by the combination of dielectric or metallic band-pass mirrors and transmission through a thin metal foil[31]. The 150 nm molybdenum or palladium foil also compensates for the intrinsic frequency chirp of the high-harmonic radiation[32] in the cut-off region of the generated spectrum, allowing to obtain near Fourier-limited attosecond pulses. Our isolated attosecond pulses have central photon energies of 94 [97, 108 and 113] eV (Fig. 2A) with an intensity full-width-at-half-maximum duration of 230 [180, 180, and 130] attoseconds, respectively. A dispersion-free interferometric setup allows to raster scan the relative timing between the laser and attosecond pulses[33]. A grazing incidence toroidal mirror focusses both pulses collinearly onto an effusive jet of helium ($\rho \sim 10^{15}$ atoms/cm$^3$). The powerful laser source, optimized HHG parameters and the use of grazing incidence optics to transport the XUV radiation yields $> 2 \times 10^7$ photons (0.3 nJ) on target per attosecond pulse. This flux enables time-resolved spectroscopy even on samples with low absorption cross section.

The attosecond (pump) pulse ionizes a fraction of the helium atoms and the momentum of the released photoelectrons is measured by a time-of-flight spectrometer (for spectra

and details of the energy conversion see supporting information (SI) available online). Depending on the relative arrival time of the two pulses, the laser electric field (probe pulse) imparts a characteristic momentum shift on the outgoing photoelectron. Detection of the final electron momentum along the axis of laser polarization for different relative delay times between the attosecond pulse and the streaking laser field yields a spectrogram with contributions from both the direct photoionization and the shake-up channels as shown in Fig. 1, right panel. To compensate for the difference in relative photoabsorption cross section[34], an electrostatic einzel-lens assembly is used to selectively increase the electron spectrometer's energy dependent acceptance angle. We recorded ~35 spectrograms for each central photon energy (representative raw-data and details of the analysis methods can be found in the SI). The data analysis is based on fitting a strong-field-solution of the time-dependent Schrödinger equation to each spectrogram[2] with first-guess wavepackets for the reconstruction composed according to electron yield measurements performed at synchrotrons[26] convoluted with the attosecond pulse bandwidth (Fig. 2**a**). The semi-infinite dressing laser field integral, corresponding to the laser vector potential in the Coulomb gauge, $A(t) = -\int_{-\infty}^{t} E(t')dt'$ is pre-determined from a first-momentum fit to the individual electron spectra. The photon-energy dependence of the absorption cross section and the small residual chirp of the attosecond pulses are accounted for in the data processing[35].

Attosecond streaking applied to helium is capable of recording the *relative* timing difference between direct and shake-up photoionization. The findings are summarized in Fig. 2**b**, grey dots and error bars represent the experimental results for the relative timing difference between the ionization channels. The methodological refinements reported here allow extracting this quantity with unprecedented precision and yield an additional advance of the shake-up wavepacket of 12.6±1.0 as at 93.9 eV photon energy

[10.6±0.9 as at 97.2 eV, 5.0±1.0 as at 108.2 eV and 4.9±1.6 as at 113.0 eV] as compared to photoemission without shake-up.

To contrast the experimental observations with fully correlated quantum mechanical modelling[36,37] we solve the time-dependent two-electron Schrödinger equation in its full dimensionality including all inter-particle interactions. Our computational method is based on accurate state-of-the-art discretization and propagation schemes (see SI) and has been successfully applied to various problems[12,37]. The computations are performed for central photon energies of 90, 95, 100, 110 and 120 eV and a full-width-at-half-intensity-maximum duration of 200as and yield theoretical spectrograms that are analysed using the identical retrieval algorithm applied to extract timing information from the experimental data (black squares in Fig. **2b**). Table 1 compares the theoretical and experimental results for the delay $\Delta\tau = \tau_{SU} - \tau_d$ between the release time $\tau_d$ of direct photoelectrons and the timing $\tau_{SU}$ of photoelectron emission accompanied by excitation of the shake-up manifold.

The remarkable agreement within the sub-attosecond standard error excludes systematic errors in the complex experiments and sophisticated numerical simulations.

With this confirmation, we can employ the theoretical treatment to determine also the *absolute* timing of photoemission from the relative measurement with sub-attosecond precision.

## Absolute zero of time in the photoelectric effect

Since in the computations the arrival time of the attosecond pulse is precisely known, the energy dependent *absolute* photoemission delay $\tau_d$ for direct photoionization can be accurately determined from the numerically simulated spectrograms which include electronic correlations to full extent (black circles, Fig. 2**b**). An alternative time-

independent fully correlated quantum simulation (grey dashed line, Fig 2b) and a single-active electron modelling of the absolute time shift in photoemission with an effective potential based on the Hartree (mean-field) approximation (black dotted line, Fig 2b) yield virtually identical results highlighting the validity of a single-photon-single-electron description and the absence of significant electronic correlation effects for this ionization channel.

We find absolute temporal shifts $\tau_d$ of -4 to -6 attoseconds in the range of examined photon energies, corresponding to a temporal advance of the photoelectron wavepacket relative to the intensity maximum of the attosecond pulse. This time shift is accumulated by the outgoing wavepacket during its formation and propagation in the attractive ionic potential. The magnitude of the time-shift corresponds to the Eisenbud-Wigner-Smith (EWS) delay $\tau_{EWS}$, which describes the temporal behaviour of the (half-)scattering event in the ionic potential, and an additional modification $\tau_{CLC}$ (Coulomb-laser-coupling) due to the long range part of the ionic Coulomb potential which is dressed by the probing laser field[6,38]. Both contributions can be independently determined (see SI) and the combined contribution yields the direct photoemission delay $\tau_d = \tau_{EWS} + \tau_{CLC}$, (grey dashed line in Fig 2b) which agrees to remarkable precision with the time-shifts extracted from the simulated spectrograms.

The absolute release time of the shake-up photoemission corresponds to the sum of $\tau_d$ and $\Delta\tau$ and can, in analogy to $\tau_d$, be decomposed into different, independent contributions. In addition to the EWS and CLC time shifts, shake-up ionization is sensitive to an additional component due to the correlation between the emitted and the remaining electron in the presence of the probing IR field.

## Correlation induced time-shift

In contrast to neutral helium and the $He^+$ $1s^1$ ionic ground state, where the electrons are deeply bound and possess no dipole moment and thus are insusceptible to the laser dressing field, the excited Rydberg states of the ion resulting from the shake-up transitions are strongly polarizable by the field due to their large spatial extent. The ionic eigenstates are assembled of a set of degenerate field-free sub-states of different orbital symmetries (e.g. 2*s* and 2*p* for n=2) which are energy-shifted in the laser electric field resulting in the lifting of the degeneracy. The counterintuitive appearance of the DC-Stark-effect induced by the rapidly oscillating (AC) electric field of the laser with $\frac{2\pi}{\omega_{laser}} = 2.7$ fs period, is a consequence of the temporal confinement of the photoelectron emission to the attosecond pulse duration. Since the dressing laser field amplitude is approximately constant during the temporal extent of the emanating electron wavepacket, the degeneracy of the field-free sub-states for each n is lifted by the instantaneous electric field.

Detection of the emitted electron in a particular direction breaks the inversion symmetry of the correlated two-electron system as shown by the electron density distributions of the asymmetric ionic states n=2 and n=3 plotted in Fig. 3. As consequence of this asymmetry these states exhibit a finite, time dependent dipole moment at the instant of photoemission.

The resulting effective dipole of the symmetry-broken singly charged ion exerts a back action on the outgoing electron leading to a time shift of the emitted electron that is included in the fully correlated two-electron EWS delay. The additional presence of an (arbitrarily weak) probing laser field amends the total observed time shift $\tau_{su}$ for electrons leaving behind helium ions in a shake-up state by an additional contribution

$\tau_{e-e}$ due to the correlation between the emitted and the remaining electron in the presence of the IR field. Accordingly,

$$\tau_{su} = \tau_{EWS} + \tau_{CLC} + \tau_{e-e}.$$

While the streaking momentum shift follows the vector potential, the additional modification of the ionic energy levels due to the Stark effect follows the instantaneous dressing laser electric field. This quarter period phase lag results in an additional contribution to the photoemission delay governed by the effective dipole moment $d_{eff}$ of the ion in the shake up state and the momentum $p_0$ of the photoelectron[12]

$$\tau_{e-e} = \frac{1}{\omega_{laser}} \tan^{-1}\left(d_{eff}\frac{\omega_{laser}}{p_0}\right) .$$

Since vector potential and electric field scale identically, the phase lag and the resulting correlation time $\tau_{e-e}$ are expected to be independent of the streaking laser field amplitude within the range of laser field amplitudes accessible to attosecond streaking (~0.1 – 2 V/Å). By contrast, the induced dipole moment in the non-degenerate atomic/ionic ground state (AC-Stark effect) scales quadratically with the laser electric field and therefore does not cause a modification of the photoemission timing.

As a major advance of this work we can isolate the correlation time from the total observed time shift, since both $\tau_{EWS}$ and $\tau_{CLC}$ can be extracted from a rigorous time-independent calculation. Isolating the n=2 state from the ensemble of shake-up states we find the contribution of electronic correlations in the presence of the laser electric field to be as large as $\tau_{e-e} = 6$ attoseconds as shown in Fig. 4**a** (for details see SI). This correlation time exhibits a weaker dependence on the excitation photon energy than the total observed time shift and it manifests itself as additional retardation of the outgoing wavepacket due to the multi-electron dynamics that is mediated by the spatially unbalanced charge density distribution of the ion after electron emission in the direction set by the detector. Since the correlation time is the time domain sequitur of the

asymmetric ionic state polarization shown in Fig. 3 we can use $\tau_{e-e}$ to experimentally determine the effective dipole moment $d_{eff}$ for the correlated shake-up wavepacket for the lowest principal quantum numbers. The results for a helium ion in the first excited state (n=2) are summarized in Fig. 4**a**. Since the charge density asymmetry of the excited ion plotted in Fig. 3 exhibits only a weak dependence on the excess energy of the outgoing photoelectron, the value for $d_{eff}$ is expected to be almost independent of the excitation energy. We find a nearly photon energy independent value of the dipole moment of $d_{eff}^{n=2} = 0.32 \pm 0.15$ a.u. in close agreement with the ab-initio simulation.

## Complete wavepacket reconstruction

Since both electrons are initially co-localized in the same atom, the outgoing photoelectron and the ion form a fully entangled quantum system. As a consequence of this entanglement, detection of the timing of the outgoing photoelectron thus reveals information about the evolving wave packet and the dynamics of the residual ionic state in a non-destructive measurement.

The magnitude of $d_{eff}^{n=2}$ crucially depends on the occupation of the different n=2 sub-states $\Psi_{n=2} = c_{2s}\Psi_{2s} + c_{2p}\Psi_{2p}$. In turn, by extracting $d_{eff}^{n=2}$ from the precise timing recorded in an attosecond streaking experiment, information on the relative phase $\Delta\varphi$ between the amplitudes $c_{2s}$ and $c_{2p}$ of the wavepacket becomes accessible. The effective dipole moment depends on the relative transition probability $\left|c_{2s}/c_{2p}\right|^2$ into the different sub-states and their relative phase $\Delta\varphi$ according to

$$d_{eff}^{n=2} = 2\, d_{+}^{n=2} \cos(\Delta\varphi) \frac{\left|c_{2s}/c_{2p}\right|}{1 + \left|c_{2s}/c_{2p}\right|^2}$$

where $d_+^{n=2} = {}^3/_2\, a.u.$ denotes the maximum dipole moment of an electron in the $n = 2$ shell.

After the state superposition is prepared by the arrival of the attosecond pulse and photoelectron ejection, the ionic quantum state evolves in time. With the relative transition probabilities known from static experiments[39], the temporal dynamics of the ionic wavepacket can be determined, provided that phase difference $\Delta\varphi$ is known. The attosecond streaking experiment yields the missing phase information. For the values of the correlation delay $\tau_{e-e}$ reported here we find $\Delta\varphi$= 1.35 ± 0.17 rad, constant within the standard error for all investigated XUV photon energies. The experimental determination of $\Delta\varphi$ allows to completely reconstruct the n=2 wavepacket (up to a global phase factor) and predict its time evolution after photoemission.

The attosecond XUV pulse with a spectral bandwidth (Fig. 2**a**) large compared to the energy difference of individual shake-up states excites multiple shake-up resonances at once and launches a fully coherent electronic wavepacket which features rapid multi-state quantum beatings. Furthermore, the presence of the laser field causes nontrivial coupling of higher shake-up channels. In this case, the unambiguous extraction of all relevant wave packet phases is hindered. A spectrally narrow XUV pulse and a longer wavelength dressing field, however, permit the spectral isolation of the n=3 shake-up peak as we show by a numerical streaking simulation in the SI. In this setting, the correlation time $\tau_{e-e}$ is again found to be accurately predicted by $d_{eff}^{n=3}$ though only partial reconstruction of the n=3 shake-up wavepacket can be achieved.

However, since the laser dressing of the photoelectron kinetic energy in the attosecond streak camera concept closely resembles frequency-resolved optical gating (FROG) techniques[40] used to determine the temporal characteristics of ultrashort laser pulses, analysis of the experimental spectrograms can likewise determine the temporal and

spectral phase characteristics of the emitted wavepackets[35]. This is of particular interest in the case of helium where the comparison of the extracted spectral phase for the different ionization channels provides energy resolved access to the role of multi-electron dynamics in the photoelectric effect that manifests itself in the reshaping of the outgoing photoelectron wavepacket. In Fig. 4**b** the group delay difference resulting from a FROG analysis of the recorded spectrograms at 97eV excitation energy is displayed (details of the analysis and the adaptive algorithm are given in the SI). Analogous analysis of the ab-initio computations shows that the spectral phase of the electron wavepacket leaving the ion in its ground state coincides within the accuracy of our retrieval method to the phase evolution ("chirp") of the exciting attosecond pulse aside from a deviation due to Coulomb-laser coupling smaller than 0.15as/eV and not exceeding 3as over the whole energy range. The green dash-dotted line in Fig. 4**b** reveals a small residual chirp of the attosecond pulse becoming visible in the reconstructed group delay (GD) for the helium 1s photo emission. By using this signal as reference, we find that the wave-packet reconstructed for the shake-up process, by contrast, carries a significant spectral chirp which is associated to the variation of the quantum phase of the wavepacket in the correlated bound-free transition. Computing the difference between the two curves removes the small residual attosecond pulse chirp which affects both channels identically and yields a sweeping group delay difference ΔGD across the bandwidth of the excitation. The comparison to the group delay behavior extracted from the ab-initio spectrograms shows a remarkable agreement over the entire spectral range (Fig. 4**b**) highlighting the effectiveness of the ab-initio computations to reproduce subtle multi-electron influences and the accuracy of the present experiment. Responsible for the temporal transformation of the debouching wavepacket is both the

photon energy dependence of the Coulomb-laser coupling and the electron correlation in the excitation process of the shake-up state.

We have experimentally shown the complete characterization of the shake-up photoionization dynamics and provide a novel benchmark for the test and development of alternative multi-electron theories for more complex systems by spectrally resolved exploration of the group delay of the outgoing photoelectron wavepacket and the Coulomb-laser coupling. Experiments at this level of precision will also provide a novel set of bounds on the controversially debated possibility of non-instantaneous electron tunneling through strong-field modified Coulomb barriers[41–43].

Based on the findings presented here, helium can serve as a tracer system for the determination of the absolute zero of time in photoemission in future experiments. By adding helium into a gas mixture or by simultaneous detection of photoelectron emission or transient XUV absorption signatures from solid state systems this capability will be available for virtually any system that can be subjected to attosecond spectroscopy. In a second step, such referential investigations will allow to replace helium by a referencing species that exhibits a significantly higher photo absorption cross section or a binding energy best suited for the excitation wavelength available in the experiment and thus proliferate sub-attosecond absolute timing precision across ultrafast spectroscopy.

## Acknowledgements

We acknowledge insightful comments and generous infrastructural support from F. Krausz. This work was supported by the Max Planck Society, the Deutsche Forschungsgemeinschaft Cluster of Excellence: Munich Centre for Advanced Photonics (http://www.munich-photonics.de), the Austrian Science Foundation project NEXTLITE

(F049 and P23359-N16) and LASERLAB-EUROPE (grant agreement no. 654148, European Union's Horizon 2020 research and innovation programme). J.F. acknowledges funding by the European Research Council (ERC-2011-AdG Proposal 290981). R.K. acknowledges a Consolidator Grant from the European Research Council (ERC-2014-CoG AEDMOS). M.S. was supported by a Marie Curie International Outgoing Fellowship (FP7-PEOPLE-2011-IOF). The computational results presented have been achieved (in part) using the Vienna Scientific Cluster (VSC).

## Author contributions

Experimental studies and analysis of experimental and theoretical signatures were carried out by M.O., F.S., V.S., A.S., T.L. and M.S.. Theory and modelling were performed by R.P, supported by S.N., J.F. and supervised by J.B.. Customized XUV optics were provided by A.G.. The manuscript was written by M.O., F.S. and M.S. All authors discussed the results and commented on the paper.

## Competing financial interests

The authors declare no competing financial interests.

## Additional information

Supplementary information, details of the analysis, histograms and representative raw-data to validate alternative data analysis methods is available in the online version of the paper.

## List of References

1. Einstein, A. Über einen die Erzeugung und Verwandlung des Lichtes betreffenden

heuristischen Gesichtspunkt. *Ann. Phys.* **322,** 132–148 (1905).

2. Schultze, M. *et al.* Delay in photoemission. *Science* **328,** 1658–62 (2010).
3. Klünder, K. *et al.* Probing Single-Photon Ionization on the Attosecond Time Scale. *Phys. Rev. Lett.* **106,** (2011).
4. Eckle, P. *et al.* Attosecond ionization and tunneling delay time measurements in helium. *Science* **322,** 1525–9 (2008).
5. Palatchi, C. *et al.* Atomic delay in helium, neon, argon and krypton. *J. Phys. B At. Mol. Opt. Phys.* **47,** 245003 (2014).
6. Wigner, E. P. Lower Limit for the Energy Derivative of the Scattering Phase Shift. *Phys. Rev.* **98,** 145–147 (1955).
7. Eisenbud, L. The Formal Properties of Nuclear Collisions. (Princeton University, 1948).
8. Smith, F. T. Lifetime matrix in collision theory. *Phys. Rev.* **118,** 349–356 (1960).
9. Nussenzveig, H. M. Time Delay in Quantum Scattering. *Phys. Rev. D* **6,** 1534–1542 (1972).
10. de Carvalho, C. A. A. & Nussenzveig, H. M. Time delay. *Phys. Rep.* **364,** 83–174 (2002).
11. Sassoli de Bianchi, M. Time-delay of classical and quantum scattering processes: a conceptual overview and a general definition. *Open Phys.* **10,** (2012).
12. Pazourek, R., Feist, J., Nagele, S. & Burgdörfer, J. Attosecond streaking of correlated two-electron transitions in helium. *Phys. Rev. Lett.* **108,** 163001 (2012).
13. Dahlström, J. M., L'Huillier, A. & Maquet, A. Introduction to attosecond delays in photoionization. *J. Phys. B At. Mol. Opt. Phys.* **45,** 183001 (2012).
14. Nagele, S., Pazourek, R., Feist, J. & Burgdörfer, J. Time shifts in photoemission from a fully correlated two-electron model system. *Phys. Rev. A* **85,** 033401 (2012).

15. Kheifets, A. S. Time delay in valence-shell photoionization of noble-gas atoms. *Phys. Rev. A* **87,** 063404 (2013).

16. Zhang, C.-H. & Thumm, U. Streaking and Wigner time delays in photoemission from atoms and surfaces. *Phys. Rev. A* **84,** (2011).

17. Zhang, C.-H. & Thumm, U. Electron-ion interaction effects in attosecond time-resolved photoelectron spectra. *Phys. Rev. A* **82,** 043405 (2010).

18. Camus, N. *et al.* Attosecond correlated dynamics of two electrons passing through a transition state. *Phys. Rev. Lett.* **108,** 073003 (2012).

19. Sukiasyan, S., Ishikawa, K. L. & Ivanov, M. Attosecond cascades and time delays in one-electron photoionization. *Phys. Rev. A* **86,** 033423 (2012).

20. Moore, L. R., Lysaght, M. A., Parker, J. S., van der Hart, H. W. & Taylor, K. T. Time delay between photoemission from the 2 p and 2 s subshells of neon. *Phys. Rev. A* **84,** 061404 (2011).

21. Baggesen, J. C. & Madsen, L. B. Polarization Effects in Attosecond Photoelectron Spectroscopy. *Phys. Rev. Lett.* **104,** (2010).

22. Baggesen, J. C. & Madsen, L. B. Erratum: Polarization Effects in Attosecond Photoelectron Spectroscopy [Phys. Rev. Lett. 104, 043602 (2010)]. *Phys. Rev. Lett.* **104,** (2010).

23. Baggesen, J. C. & Madsen, L. Atomic and molecular phases through attosecond streaking. *Phys. Rev. A* **83,** (2011).

24. Kheifets, A. S., Saha, S., Deshmukh, P. C., Keating, D. A. & Manson, S. T. Dipole phase and photoelectron group delay in inner-shell photoionization. *Phys. Rev. A* **92,** 063422 (2015).

25. Nagele, S. *et al.* Time-resolved photoemission by attosecond streaking: extraction of time information. *J. Phys. B At. Mol. Opt. Phys.* **44,** 081001 (2011).

26. Heimann, P. A. *et al.* Helium and neon photoelectron satellites at threshold. *Phys. Rev. A* **34,** 3782–3791 (1986).

27. Itatani, J. *et al.* Attosecond Streak Camera. *Phys. Rev. Lett.* **88,** (2002).

28. Schweinberger, W. *et al.* Waveform-controlled near-single-cycle milli-joule laser pulses generate sub-10 nm extreme ultraviolet continua. *Opt. Lett.* **37,** 3573–5 (2012).

29. Corkum, P. B. Plasma perspective on strong-field multiphoton ionization. *Phys. Rev. Lett.* **71,** 1994–1997 (1993).

30. Schafer, K. & Kulander, K. High Harmonic Generation from Ultrafast Pump Lasers. *Phys. Rev. Lett.* **78,** 638–641 (1997).

31. Hofstetter, M. *et al.* Lanthanum–molybdenum multilayer mirrors for attosecond pulses between 80 and 130 eV. *New J. Phys.* **13,** 063038 (2011).

32. Mairesse, Y. *et al.* Attosecond synchronization of high-harmonic soft x-rays. *Science* **302,** 1540–3 (2003).

33. Fiess, M. *et al.* Versatile apparatus for attosecond metrology and spectroscopy. *The Rev. Sci. Instrum.* **81,** 093103 (2010).

34. Becker, U. & Shirley, D. A. *VUV and Soft X-ray Photoionization*. (Springer Science & Business Media, 2012).

35. Yakovlev, V. S., Gagnon, J., Karpowicz, N. & Krausz, F. Attosecond streaking enables the measurement of quantum phase. *Phys. Rev. Lett.* **105,** 073001 (2010).

36. Feist, J. *et al.* Nonsequential two-photon double ionization of helium. *Phys. Rev. A* **77,** 043420 (2008).

37. Schneider, B. I. *et al.* in *Quantum Dynamic Imaging* 149–208 (Springer, 2011).

38. Ivanov, M. & Smirnova, O. How accurate is the attosecond streak camera? *Phys. Rev. Lett.* **107,** 213605 (2011).

39. Woodruff, P. R. & Samson, J. A. R. Measurements of partial cross sections and autoionization in the photoionization of helium to He+ (N=2). *Phys. Rev. A* **25,** 848–856 (1982).

40. Trebino, R. *et al.* Measuring ultrashort laser pulses in the time-frequency domain using frequency-resolved optical gating. *Rev. Sci. Instrum.* **68,** 3277 (1997).

41. Pedatzur, O. *et al.* Attosecond tunnelling interferometry. *Nat. Phys.* **11,** 815–819 (2015).

42. Torlina, L. *et al.* Interpreting attoclock measurements of tunnelling times. *Nat. Phys.* **11,** 503–508 (2015).

43. Landsman, A. S. & Keller, U. Tunnelling time in strong field ionisation. *J. Phys. B At. Mol. Opt. Phys.* **47,** 204024 (2014).

44. Ramachandran, P. & Varoquaux, G. Mayavi: 3D Visualization of Scientific Data. *Comput. Sci. Eng.* **13,** 40–51 (2011).

# Figure Captions

**Fig. 1** Attosecond streaking spectroscopy of shake-up states in helium.

Photoemission of an electron from the helium ground state with a binding energy of 24.6 eV results in the liberation of the electron with a kinetic energy equal to the difference between photon- and binding-energy into the ionization continuum (middle panel). The ionic potential rearranges as result of the electron loss due to the modified screening of the nucleus and the remaining electron occupies a more tightly bound state (shake-down or direct photoemission).

Alternatively, the electron emission can be accompanied by the excitation of the remaining electron into one out of a series of shake-up states n (right panel). Due to electronic correlation the escaping electron's kinetic energy gets reduced by the excitation energy $\Delta E_{su}$.

In the presence of a time delayed dressing laser field the kinetic energy distribution of both quantum pathways is modulated according to the attosecond streak camera principle permitting an accurate comparison of the electron release times.

**Fig. 2** Absolute timing of the photoelectric effect in helium

The timing difference between the direct helium 1s and the shake-up electron emission is determined experimentally at central photon energies of 93.9, 97.2, 108.2 and 112.8 eV. The relative spectral intensity, bandwidth and duration of the attosecond pulses are displayed in panel a. Vertical arrows in the panel b indicate the observed relative timing and the vertical error bars denote the standard error of the mean determined from a set of measurements (N~35). Horizontal error bars indicate the experimental uncertainty in the energy determination. Black circles depict the ab-initio modelling results for the absolute photoemission delay of the shake-down process, the grey dashed line shows

the result of a fully correlated but time independent prediction and coincides with the predictions of a single-active electron model (black dotted line). Ab-initio results for the shake-up ensemble photoemission delay are shown as black squares, together with a cubic-spline-fit to guide the eye (grey dash-dotted line).

**Fig. 3** DC-Stark-effect at optical frequencies.

False color plot[44] of the electronic density distribution in the excited helium ionic n=2 and n=3 state after emission of a photoelectron. Discrimination of the detection direction (indicated by the arrow labeled "Detector") results in an asymmetric charge density distribution carrying an effective dipole moment $d_{eff}$ that couples to the laser electric field which is approximately static in space and time for the duration of the attosecond pulse triggering the photoemission.

**Fig. 4** Effective dipole moment for n=2 and relative group delay dispersion of the correlation time.

a) Correlation delay $\tau_{e-e}$ as a function of the photon energy of the attosecond pulse and the derived effective dipole moment $d_{eff}^{n=2}$ of the excited ionic state (right ordinate). Blue dash-dotted line: Theoretical prediction for $d_{eff}^{n=2}$ based on ab-initio modelling.

b) Frequency resolved analysis of the recorded spectrograms within the bandwidth of the attosecond pulse (indicated by the grey dotted line). While the temporal phase of the He 1s photoelectrons is almost constant across the attosecond pulse bandwidth (green dash-dotted line shows group delay), the shake-up photoelectron wavepacket exhibits significant spectral chirp visible as sweeping group delay difference (ΔGD). The red dashed line indicates ΔGD between the two channels computed from the experimental

results (shaded area displays the confidence interval) in comparison to the theoretical result (blue line).

Within the bandwidth of the attosecond pulse (here centered at 97 eV) the measured group delay difference decreases as function of photon energy.

# Tables

**Table 1** Time shift $\Delta\tau$ between direct and shake-up photoemission in helium for different photon energies.

| Photon-energy [eV] | Δτ Experiment [$10^{-18}$ s] | Standard error [$10^{-18}$ s] | Δτ Theory [$10^{-18}$ s] |
|---|---|---|---|
| 93.9 | -12.6 | 0.99 | -13.3 |
| 97.2 | -10.6 | 0.85 | -10.6 |
| 108.2 | -5.0 | 1.01 | -6.0 |
| 113.0 | -4.9 | 1.60 | -4.8 |

# Figures

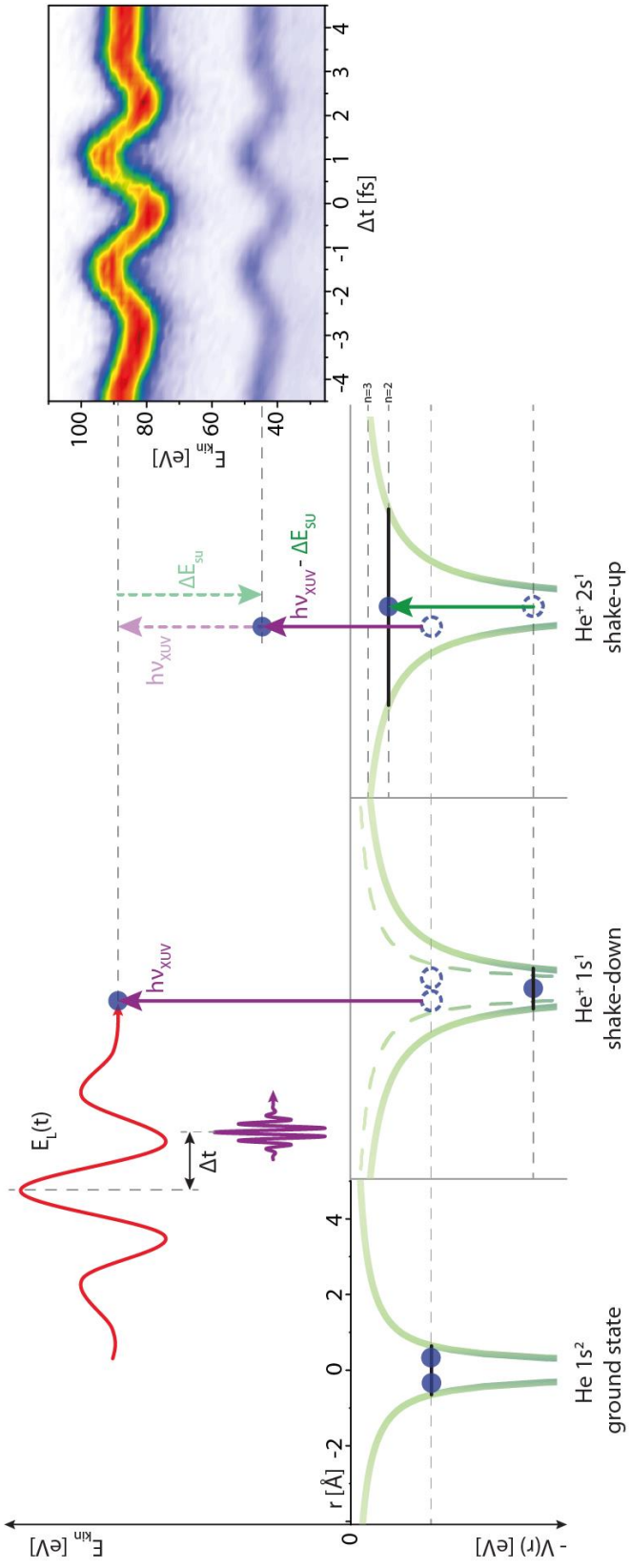


Fig. 1

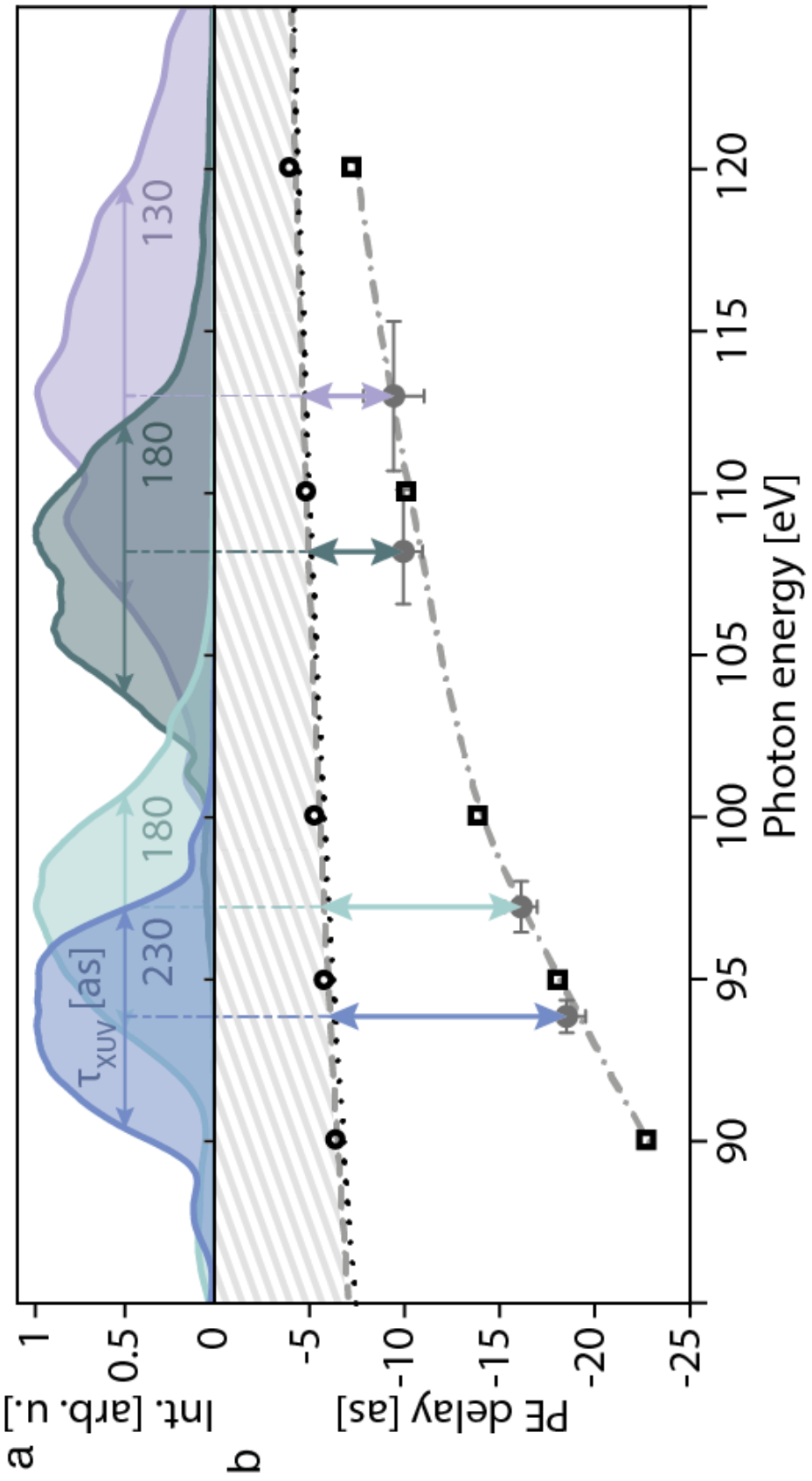
a
Int. [arb. u.]
1
0.5
0
b
PE delay [as]
-5
-10
-15
-20
-25
90
95
100
105
110
115
120
Photon energy [eV]
$\tau_{XUV}$ [as]
230
180
180
130

Fig. 2

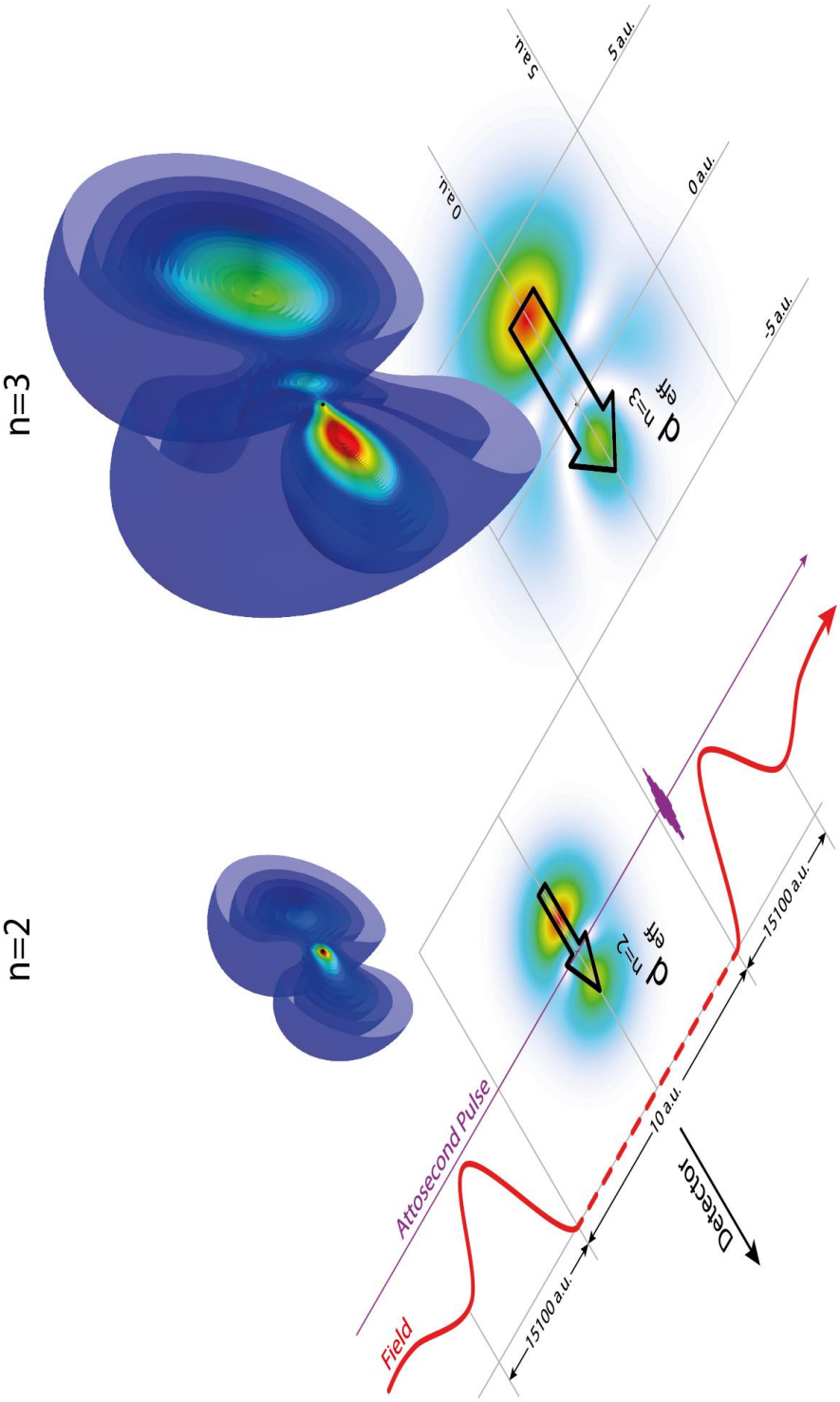
n=3
n=2
d n=3 eff
d n=2 eff
5 a.u.
0 a.u.
-5 a.u.
Attosecond Pulse
Field
15100 a.u.
10 a.u.
15100 a.u.
Detector

Fig. 3

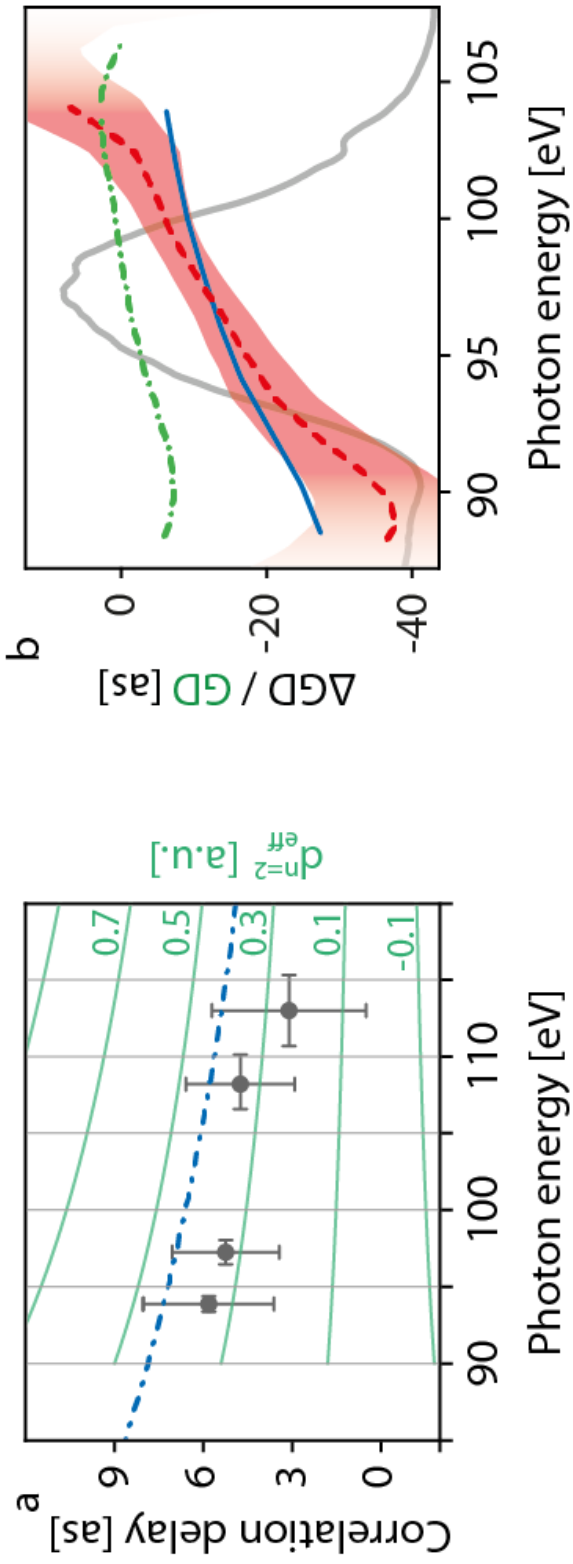
b
ΔGD / GD [as]
0
-20
-40
90
95
100
105
Photon energy [eV]
a
Correlation delay [as]
6
9
3
0
90
100
110
Photon energy [eV]
0.7
0.5
0.3
0.1
-0.1
$d_{eff}^{n=2}$ [a.u.]

Fig. 4